data

MDPI

Data Descriptor

Dataset: Impact of β-Galactosylceramidase Overexpression on the Protein Profile of Braf(V600E) Mutated Melanoma Cells

Davide Capoferri [1], Paola Chiodelli [1,†], Stefano Calza [1], Marcello Manfredi [2,3] and Marco Presta [1,4,*]

[1] Department of Molecular and Translational Medicine, University of Brescia, 25123 Brescia, Italy; davide.capoferri@unibs.it (D.C.); paola.chiodelli@unicatt.it (P.C.); stefano.calza@unibs.it (S.C.)
[2] Department of Translational Medicine, University of Piemonte Orientale, 13100 Novara, Italy; marcello.manfredi@uniupo.it
[3] Center for Allergic and Autoimmune Diseases, University of Piemonte Orientale, 13100 Novara, Italy
[4] Consorzio Interuniversitario Biotecnologie (CIB), Unit of Brescia, 25123 Brescia, Italy
* Correspondence: marco.presta@unibs.it
† Present address: Dipartimento di Scienze della Vita e Sanità Pubblica, Università Cattolica del Sacro Cuore, 00168 Rome, Italy.

Abstract: β-Galactosylceramidase (GALC) is a lysosomal enzyme involved in sphingolipid metabolism by removing β-galactosyl moieties from β-galactosyl ceramide and β-galactosyl sphingosine. Previous observations have shown that GALC exerts a pro-oncogenic activity in human melanoma. Here, the impact of GALC overexpression on the proteomic landscape of *BRAF*-mutated A2058 and A375 human melanoma cell lines was investigated by liquid chromatography–tandem mass spectrometry analysis of the cell extracts. The results indicate that *GALC* overexpression causes the upregulation/downregulation of 172/99 proteins in *GALC*-transduced cells when compared to control cells. Gene ontology categorization of up/down-regulated proteins indicates that GALC may modulate the protein landscape in *BRAF*-mutated melanoma cells by affecting various biological processes, including RNA metabolism, cell organelle fate, and intracellular redox status. Overall, these data provide further insights into the pro-oncogenic functions of the sphingolipid metabolizing enzyme GALC in human melanoma.

Dataset: The data set has been submitted as a supplement to this paper.

Keywords: melanoma; proteomics; sphingolipids; β-galactosylceramidase

Citation: Capoferri, D.; Chiodelli, P.; Calza, S.; Manfredi, M.; Presta, M. Dataset: Impact of β-Galactosylceramidase Overexpression on the Protein Profile of Braf(V600E) Mutated Melanoma Cells. *Data* **2023**, *8*, 177. https://doi.org/10.3390/data8120177

Academic Editor: Robertas Damaševičius

Received: 23 June 2023
Revised: 22 November 2023
Accepted: 23 November 2023
Published: 24 November 2023

1. Introduction

β-Galactosylceramidase (GALC; EC 3.2.1.46) is a lysosomal hydrolase that catalyzes the removal of the β-galactose moiety from β-galactosyl ceramide and other sphingolipids [1–4]. A gradual increase in *GALC* expression occurs during human melanoma progression in skin specimens ranging from common nevi to stage IV melanoma [5], thus suggesting that GALC might act as a pro-oncogenic enzyme [6–9]. In keeping with this hypothesis, *Galc* knockdown causes a decrease in the tumorigenic and metastatic potential of murine melanoma B16 cells that also showed significant alterations in their lipidomic profile, characterized by increased levels of the oncosuppressive sphingolipid ceramide [10,11]. Accordingly, increased levels of ceramide were also observed in *GALC*-silenced human melanoma A2058 cells and tumor xenografts, with a consequent decrease in their tumorigenic potential [5]. However, the mechanisms by which GALC exerts its pro-tumorigenic functions in human melanoma remain poorly understood.

Analysis of the proteome may provide valuable information for the characterization of the biological pathways leading to melanoma progression [12–16] and for the identification of diagnostic and prognostic biomarkers [17–20]. As stated above, GALC may exert a pro-oncogenic role in *Braf* wild-type murine melanoma cells [5]. However, approximately 50% of human melanomas are characterized by the BRAF (V600E) tumor driver mutation [21–26], which represents a major target in melanoma therapy [27–30]. These observations prompted us to assess the role of GALC in human melanoma in the presence of a *BRAF*-mutated background [31]. To this purpose, liquid chromatography–tandem mass spectrometry (LC-MS/MS) was used to investigate the impact of *GALC* overexpression on the proteomic profile of BRAF (V600E)-mutated A2058 and A375 human melanoma cells. Indeed, wild-type A2058 and A375 cells express intermediate levels of *GALC* mRNA and protein when compared to other human melanoma cell lines, therefore making them suitable for assessing the effect of *GALC* upregulation on the biological behavior of human melanoma cells in a *BRAF*-mutated background. In addition, given the well-known heterogeneity that characterizes human tumors [32–36], the use of two cell lines harboring the same driver mutation allows the identification of common protein profiles modulated by *GALC* overexpression in *BRAF*-mutated melanoma cells. Here, we will briefly illustrate the proteomic data that characterize the impact exerted by GALC on *BRAF*-mutated human melanoma cells. Refer to [31] for in-depth analysis and discussion of these data.

2. Data Description

A2058-upGALC and A375-upGALC cells, together with the corresponding control A2058-mock and A375-mock cells, were obtained by lentiviral infection, and *GALC* overexpression was confirmed by a semiquantitative real-time polymerase chain reaction and enzymatic activity assays [31]. Next, LC-MS/MS analysis was performed on the cell extracts of the four cell lines. The number of proteins identified with a false discovery rate (FDR) below 1% is shown in Table 1.

Table 1. Proteins identified in mock and upGALC cell lines.

Cell Line	N° of Samples	N° of Identified Proteins
A2058-mock cells	4	1471
A2058-upGALC cells	4	1583
A375-mock cells	4	1483
A375-upGALC cells	4	1482

A hierarchic analysis performed by comparing the A2058-upGALC *plus* A375-upGALC data sets to the A2058-mock *plus* A375-mock data sets demonstrated that 304 and 340 proteins are up- or down-regulated (Q value < 0.05) in upGALC vs. mock cells (Supplementary Table S1).

Next, gene ontology (GO) categorization [37–39] was performed using the Enrichr platform [40] (https://maayanlab.cloud/Enrichr/, accessed on 18 July 2023) on the 271 *GALC*-modulated proteins (172 up-regulated *plus* 99 down-regulated) characterized by a fold change greater than 1.5 or lower than 0.67. The analysis identified the terms "RNA binding" (p value = 2.01×10^{-12}) and "intracellular organelle/secretory granule lumen" (p value = 1.17×10^{-12}) as the most enriched GO molecular function and GO cellular component terms, respectively, whereas "tricarboxylic acid cycle" represented a highly enriched Kyoto Encyclopedia of Genes and Genomes (KEGG) pathway [41] (p value = 2.59×10^{-4}). Accordingly, string analysis of the differentially expressed proteins identified three major clusters (protein–protein interaction enrichment p value $\leq 1.0 \times 10^{-16}$) corresponding to the GO terms "RNA binding" (FDR = 4.11×10^{-8}), "extracellular exosomes" (FDR = 6.77×10^{-21}), and "oxidation–reduction process" (FDR = 2.79×10^{-15}) (Figure 1).

Together, the data demonstrate that the lysosomal sphingolipid metabolizing enzyme GALC exerts a significant impact on the proteomic landscape of *BRAF*-mutated human melanoma cells. At present, the biochemical mechanisms leading to the observed alterations

in the melanoma proteome induced by *GALC* upregulation remain unclarified. Previous observations had shown that *GALC* downregulation may exert significant alterations in the lipid profile of murine melanoma [5]. Further studies will be required to assess the effect of the modulation of GALC activity on the sphingolipidome of human melanoma cells and how this, in turn, may orchestrate their transcriptomic and proteomic profiles.

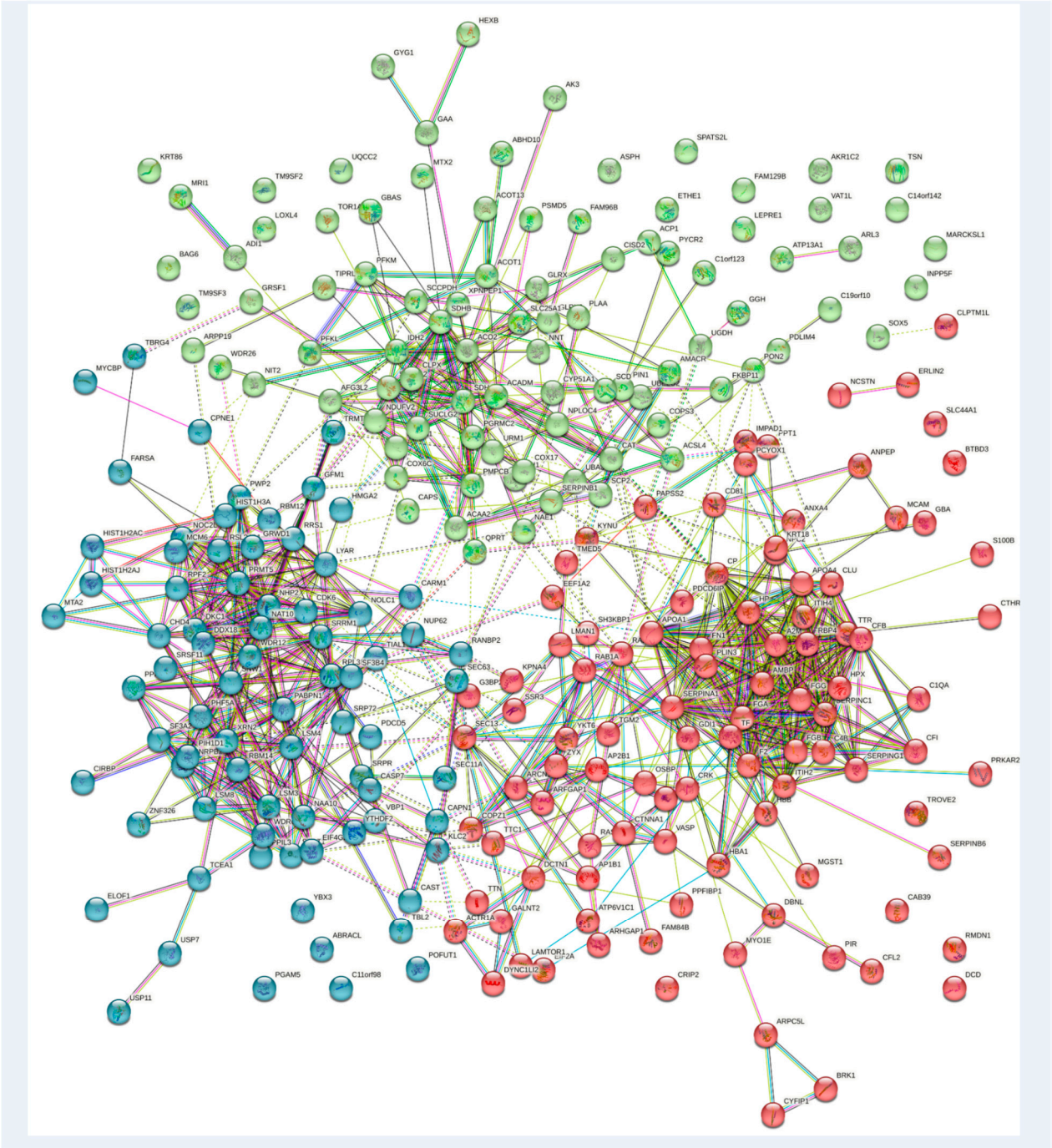

Figure 1. String analysis of GALC-modulated proteins in melanoma cells. The three clusters are defined by the GO terms "RNA binding" (in blue), "extracellular exosomes" (in red), and "oxidation–reduction process" (in green).

Data Records

The data presented in this study are available in Supplementary Table S2. Column A contains the following description of the identified protein peaks: UniProt primary

accession ID | UniProt ID, name of the protein, organism (OS), and gene (GN). Columns B–Q show the values of the normalized peak area for the four replicates of A375-upGALC (B–E), A375-mock (F-I), A2058-upGALC (J–M), and A2058-mock (N–Q) cells.

3. Materials and Methods

3.1. Cell Cultures and Lentivirus Infection

A2058 and A375 cells were purchased from the American Type Culture Collection and grown in Dulbecco's modified Eagle medium supplemented with 10% heat-inactivated fetal bovine serum, 100 U/mL penicillin, and 100 μg/mL streptomycin (Thermo Fisher Scientific, Waltham, MA, USA), hereinafter referred to as "complete medium". Cells were maintained at 37 °C and 5% CO_2 in a humidified incubator. Cells were infected with a lentivirus (Addgene plasmid #19070) harboring the human *GALC* cDNA (NM_000153.3), thus generating A2058-upGALC and A375-upGALC cells. Cells transduced with an empty vector were used as controls (A2058-mock and A375-mock cells). For the infection protocol, cells were incubated with lentiviral particles for 7 h in a complete medium containing 8.0 μg/mL of polybrene and selected by adding 1 μg/mL puromycin 24 h later. Next, *GALC* overexpression was confirmed by a semiquantitative real time polymerase chain reaction and by a GALC activity assay as previously described [5,31].

3.2. Mass Spectrometry

3.2.1. Sample Preparation

Cells were maintained for 2 days in Dulbecco's modified Eagle medium *plus* 2% heat-inactivated fetal bovine serum. Then, cell samples were lysed with a radioimmunoprecipitation assay lysis buffer, denatured with trifluoroethanol, subjected to dithiothreitol reduction (200 mM), iodoacetamide alkylation (200 mM), and complete trypsin protein digestion. The peptide digests were desalted on the Discovery® DSC-18 solid phase extraction 96-well plate (Merck KGaA, Darmstadt, Germany) (25 mg/well). After the desalting process, samples were vacuum-evaporated and reconstituted in a mobile phase for the analysis [42]. All reagents were from Sigma-Aldrich Inc. (St. Louis, MO, USA).

3.2.2. Proteomic Analysis

The digested peptides were analyzed with an Ultra High-Performance Liquid Chromatography Vanquish system (Thermo Scientific, Rodano, Italy) coupled with an Orbitrap Q-Exactive Plus (Thermo Scientific). Peptides were separated by a reverse-phase column (Accucore™ RP-MS 100 × 2.1 mm, particle size 2.6 μm) at a flow rate of 0.2 mL/min, with water and acetonitrile as mobile phase A and B respectively, both acidified with 0.1% formic acid. The analysis was performed using the following gradient: 0–5 min from 2% to 5% B; 5–55 min from 5% to 30% B; 55–61 min from 30% to 90% B and hold for one min, at 62.1 min the percentage of B was set to the initial condition of the run at 2% and held for about 8 min to equilibrate the column, for a total run time of 70 min. The MS analysis was performed in positive ion mode. The electrospray ionization source was used with a voltage of 2.8 kV. The capillary temperature, sheath gas flow, auxiliary gas, and spare gas flow were set at 325 °C, 45 arb, 10 arb, and 2, respectively. S-lens was set at 70 rf. A data-dependent (ddMS2) top-10 scan mode was used for the acquisition of spectra. Survey full-scan MS spectra (mass range m/z 381 to 1581) were acquired with resolution R = 70,000 and an automatic gain control target of 3×10^6. MS/MS fragmentation was performed using high-energy c-trap dissociation with resolution R = 35,000 and an automatic gain control target of 1×10^6. The normalized collision energy was set to 30. The injection volume was 3 μL.

The mass spectra analysis was carried out using MaxQuant software (version 1.6.14). MaxQuant parameters were set as follows: trypsin was selected for enzyme specificity; the search parameters were fixed to an initial precursor ion tolerance of 10 ppm and MS/MS tolerance at 20 ppm; as fixed modification, carbamidomethylation was set, whereas oxidation was set as variable modification. The maximum missed cleavages were set to 2. Andromeda

search engine searched the spectra in MaxQuant against the Uniprot_CP_Human_2018 sequence database. Label-free quantification was performed including a match between runs option with the following parameters: protein and peptide FDR was set to 0.01 according to standard procedures; the quantification was based on the extracted ion chromatograms, with a minimum ratio count of 1; the minimum required peptide length was set to 7 amino acids. Statistical analyses for protein peak identification were performed using MaxQuant software (version 1.6.14) and MetaboAnalyst software (version 5.0) (https://www.metaboanalyst.ca—accessed on 24 January 2021) [43].

3.3. Statistical Analysis

Peak intensity values of the identified proteins were first transformed to log scale (plus 1 to avoid zero values) and modelled using a generalized linear mixed model to account for data hierarchical structure (condition nested within cell line) using R 4.3.0. Q values were considered to identify differentially expressed proteins due to their high statistical power. Proteins with a Q value < 5% are listed in Supplementary Table S1. Among them, proteins with a change greater than 1.5 or lower than 0.67 were run in STRING [44] and clustered in GO classes.

Supplementary Materials: The following supporting information can be downloaded at https://www.mdpi.com/article/10.3390/data8120177/s1. Table S1: List of proteins differentially expressed in upGALC vs. mock cells; Table S2: Raw peak areas normalized to whole area of mock and upGALC A2058 and A375 cells.

Author Contributions: Conceptualization: D.C. and M.P.; methodology: M.M.; investigation: D.C. and P.C.; data curation: D.C.; statistical analysis: D.C. and S.C.; writing—original draft preparation: D.C. and M.P.; writing—review and editing: D.C. and M.P.; supervision: M.P.; funding acquisition: M.M. and M.P. All authors have read and agreed to the published version of the manuscript.

Funding: This research was supported in part by Associazione Italiana per la Ricerca sul Cancro (AIRC) IG Grant n. 18493, PNRR M4C2-Investimento 1.4-CN00000041 finanziato dall'Unione Europea—NextGenerationEU, and Consorzio Universitario Biotecnologie (CIB) to M.P. and by the AGING Project—Department of Excellence—DIMET, Università del Piemonte Orientale to M.M.

Institutional Review Board Statement: Not applicable.

Data Availability Statement: The data presented in this study are available in the Supplementary Material here.

Conflicts of Interest: The authors declare no conflict of interest.

Abbreviations

FDR: False Discovery Rate; GALC: β-galactosylceramidase; GO: Gene Ontology; LC-MS/MS: Liquid Chromatography–Tandem Mass Spectrometry.

References

1. Won, J.S.; Singh, A.K.; Singh, I. Biochemical, Cell biological, pathological, and therapeutic aspects of Krabbe's disease. *J. Neurosci. Res.* **2016**, *94*, 990–1006. [CrossRef] [PubMed]
2. Reza, S.; Ugorski, M.; Suchanski, J. Glucosylceramide and galactosylceramide, small glycosphingolipids with significant impact on health and disease. *Glycobiology* **2021**, *31*, 1416–1434. [CrossRef] [PubMed]
3. Deane, J.E.; Graham, S.C.; Kim, N.N.; Stein, P.E.; McNair, R.; Cachon-Gonzalez, M.B.; Cox, T.M.; Read, R.J. Insights into Krabbe disease from structures of galactocerebrosidase. *Proc. Natl. Acad. Sci. USA* **2011**, *108*, 15169–15173. [CrossRef]
4. Hill, C.H.; Cook, G.M.; Spratley, S.J.; Fawke, S.; Graham, S.C.; Deane, J.E. The mechanism of glycosphingolipid degradation revealed by a GALC-SapA complex structure. *Nat. Commun.* **2018**, *9*, 151. [CrossRef]
5. Belleri, M.; Paganini, G.; Coltrini, D.; Ronca, R.; Zizioli, D.; Corsini, M.; Barbieri, A.; Grillo, E.; Calza, S.; Bresciani, R.; et al. β-Galactosylceramidase promotes melanoma growth via modulation of ceramide metabolism. *Cancer Res.* **2020**, *80*, 5011–5023. [CrossRef]
6. Presta, M. β-Galactosylceramidase in cancer: Friend or foe? *Trends Cancer* **2021**, *7*, 974–977. [CrossRef]

7. Atilla-Gokcumen, G.E.; Muro, E.; Relat-Goberna, J.; Sasse, S.; Bedigian, A.; Coughlin, M.L.; Garcia-Manyes, S.; Eggert, U.S. Dividing cells regulate their lipid composition and localization. *Cell* **2014**, *156*, 428–439. [CrossRef]
8. Liu, D.G.; Xue, L.; Li, J.; Yang, Q.; Peng, J.Z. Epithelial-mesenchymal transition and GALC expression of circulating tumor cells indicate metastasis and poor prognosis in non-small cell lung cancer. *Cancer Biomark.* **2018**, *22*, 417–426. [CrossRef]
9. Yang, M.; Jiang, Z.; Yao, G.; Wang, Z.; Sun, J.; Qin, H.; Zhao, H. GALC Triggers Tumorigenicity of Colorectal Cancer via Senescent Fibroblasts. *Front. Oncol.* **2020**, *10*, 380. [CrossRef]
10. Young, M.M.; Kester, M.; Wang, H.G. Sphingolipids: Regulators of crosstalk between apoptosis and autophagy. *J. Lipid Res.* **2013**, *54*, 5–19. [CrossRef] [PubMed]
11. Pilatova, M.B.; Solarova, Z.; Mezencev, R.; Solar, P. Ceramides and their roles in programmed cell death. *Adv. Med. Sci.* **2023**, *68*, 417–425. [CrossRef]
12. Ruiz, E.M.; Alhassan, S.A.; Errami, Y.; Abd Elmageed, Z.Y.; Fang, J.S.; Wang, G.; Brooks, M.A.; Abi-Rached, J.A.; Kandil, E.; Zerfaoui, M. A Predictive Model of Adaptive Resistance to BRAF/MEK Inhibitors in Melanoma. *Int. J. Mol. Sci.* **2023**, *24*, 8407. [CrossRef]
13. Gao, L.; Zhu, D.; Wang, Q.; Bao, Z.; Yin, S.; Qiang, H.; Wieland, H.; Zhang, J.; Teichmann, A.; Jia, J. Proteome Analysis of USP7 Substrates Revealed Its Role in Melanoma Through PI3K/Akt/FOXO and AMPK Pathways. *Front. Oncol.* **2021**, *11*, 650165. [CrossRef]
14. Gao, L.; Zhu, D.; Wang, Q.; Bao, Z.; Yin, S.; Qiang, H.; Wieland, H.; Zhang, J.; Teichmann, A.; Jia, J. Corrigendum: Proteome Analysis of USP7 Substrates Revealed Its Role in Melanoma through PI3K/Akt/FOXO and AMPK Pathways. *Front. Oncol.* **2021**, *11*, 736438. [CrossRef] [PubMed]
15. Baruthio, F.; Quadroni, M.; Ruegg, C.; Mariotti, A. Proteomic analysis of membrane rafts of melanoma cells identifies protein patterns characteristic of the tumor progression stage. *Proteomics* **2008**, *8*, 4733–4747. [CrossRef] [PubMed]
16. Bernard, K.; Litman, E.; Fitzpatrick, J.L.; Shellman, Y.G.; Argast, G.; Polvinen, K.; Everett, A.D.; Fukasawa, K.; Norris, D.A.; Ahn, N.G.; et al. Functional proteomic analysis of melanoma progression. *Cancer Res.* **2003**, *63*, 6716–6725. [PubMed]
17. Krisp, C.; Parker, R.; Pascovici, D.; Hayward, N.K.; Wilmott, J.S.; Thompson, J.F.; Mann, G.J.; Long, G.V.; Scolyer, R.A.; Molloy, M.P. Proteomic phenotyping of metastatic melanoma reveals putative signatures of MEK inhibitor response and prognosis. *Br. J. Cancer* **2018**, *119*, 713–723. [CrossRef] [PubMed]
18. Harel, M.; Ortenberg, R.; Varanasi, S.K.; Mangalhara, K.C.; Mardamshina, M.; Markovits, E.; Baruch, E.N.; Tripple, V.; Arama-Chayoth, M.; Greenberg, E.; et al. Proteomics of melanoma response to immunotherapy reveals mitochondrial dependence. *Cell* **2019**, *179*, 236–250.e18. [CrossRef] [PubMed]
19. Militaru, I.V.; Rus, A.A.; Munteanu, C.V.A.; Manica, G.; Petrescu, S.M. New panel of biomarkers to discriminate between amelanotic and melanotic metastatic melanoma. *Front. Oncol.* **2023**, *12*, 1061832. [CrossRef]
20. Pickering, C.; Aiyetan, P.; Xu, G.; Mitchell, A.; Rice, R.; Najjar, Y.G.; Markowitz, J.; Ebert, L.M.; Brown, M.P.; Tapia-Rico, G.; et al. Plasma glycoproteomic biomarkers identify metastatic melanoma patients with reduced clinical benefit from immune checkpoint inhibitor therapy. *Front. Immunol.* **2023**, *14*, 1187332. [CrossRef]
21. Hoeflich, K.; Eby, M.; Forrest, W.; Gray, D.; Tien, J.; Stern, H.; Murray, L.; Davis, D.; Modrusan, Z.; Seshagiri, S. Regulation of ERK3/MAPK6 expression by BRAF. *Int. J. Oncol.* **2006**, *29*, 839–849. [CrossRef] [PubMed]
22. Kannengiesser, C.; Spatz, A.; Michiels, S.; Eychene, A.; Dessen, P.; Lazar, V.; Winnepenninckx, V.; Lesueur, F.; Druillennec, S.; Robert, C.; et al. Gene expression signature associated with BRAF mutations in human primary cutaneous melanomas. *Mol. Oncol.* **2008**, *1*, 425–430. [CrossRef] [PubMed]
23. Sheridan, C.; Brumatti, G.; Martin, S.J. Oncogenic B-RafV600E inhibits apoptosis and promotes ERK-dependent inactivation of Bad and Bim. *J. Biol. Chem.* **2008**, *283*, 22128–22135. [CrossRef]
24. Cui, Y.; Borysova, M.K.; Johnson, J.O.; Guadagno, T.M. Oncogenic B-Raf(V600E) induces spindle abnormalities, supernumerary centrosomes, and aneuploidy in human melanocytic cells. *Cancer Res.* **2010**, *70*, 675–684. [CrossRef]
25. Ottaviano, M.; Giunta, E.F.; Tortora, M.; Curvietto, M.; Attademo, L.; Bosso, D.; Cardalesi, C.; Rosanova, M.; De Placido, P.; Pietroluongo, E.; et al. BRAF Gene and Melanoma: Back to the Future. *Int. J. Mol. Sci.* **2021**, *22*, 3474. [CrossRef] [PubMed]
26. Cancer Genome Atlas Network. Genomic Classification of Cutaneous Melanoma. *Cell* **2015**, *161*, 1681–1696. [CrossRef] [PubMed]
27. Ascierto, P.A.; Kirkwood, J.M.; Grob, J.-J.; Simeone, E.; Grimaldi, A.M.; Maio, M.; Palmieri, G.; Testori, A.; Marincola, F.M.; Mozzillo, N. The role of BRAF V600 mutation in melanoma. *J. Transl. Med.* **2012**, *10*, 85. [CrossRef]
28. Castellani, G.; Buccarelli, M.; Arasi, M.B.; Rossi, S.; Pisanu, M.E.; Bellenghi, M.; Lintas, C.; Tabolacci, C. BRAF Mutations in Melanoma: Biological Aspects, Therapeutic Implications, and Circulating Biomarkers. *Cancers* **2023**, *15*, 4026. [CrossRef]
29. Van Akkooi, A.C.; Hauschild, A.; Long, G.V.; Mandala, M.; Kicinski, M.; Govaerts, A.S.; Klauck, I.; Ouali, M.; Lorigan, P.C.; Eggermont, A.M. COLUMBUS-AD: Phase III study of adjuvant encorafenib + binimetinib in resected stage IIB/IIC BRAF V600-mutated melanoma. *Future Oncol.* **2023**, *19*, 2017–2027. [CrossRef]
30. Kim, S.; Kim, H.T.; Suh, H.S. Combination therapy of BRAF inhibitors for advanced melanoma with BRAF V600 mutation: A systematic review and meta-analysis. *J. Dermatol. Treat.* **2018**, *29*, 314–321. [CrossRef]
31. Capoferri, D.; Chiodelli, P.; Corli, M.; Belleri, M.; Scalvini, E.; Mignani, L.; Guerra, J.; Grillo, E.; De Giorgis, V.; Manfredi, M.; et al. The pro-oncogenic sphingolipid-metabolizing enzyme β-galactosylceramidase modulates the proteomic landscape in BRAF(V600E)-mutated human melanoma cells. *Int. J. Mol. Sci.* **2023**, *24*, 10555. [CrossRef] [PubMed]
32. Ng, M.F.; Simmons, J.L.; Boyle, G.M. Heterogeneity in Melanoma. *Cancers* **2022**, *14*, 3030. [CrossRef] [PubMed]

33. Lee, D.; Park, Y.; Kim, S. Towards multi-omics characterization of tumor heterogeneity: A comprehensive review of statistical and machine learning approaches. *Brief. Bioinform.* **2021**, *22*, bbaa188. [CrossRef] [PubMed]
34. Donnelly, D., 3rd; Aung, P.P.; Jour, G. The "-OMICS" facet of melanoma: Heterogeneity of genomic, proteomic and metabolomic biomarkers. *Semin. Cancer Biol.* **2019**, *59*, 165–174. [CrossRef] [PubMed]
35. Grzywa, T.M.; Paskal, W.; Wlodarski, P.K. Intratumor and Intertumor Heterogeneity in Melanoma. *Transl. Oncol.* **2017**, *10*, 956–975. [CrossRef]
36. Fisher, R.; Pusztai, L.; Swanton, C. Cancer heterogeneity: Implications for targeted therapeutics. *Br. J. Cancer* **2013**, *108*, 479–485. [CrossRef]
37. Ashburner, M.; Ball, C.A.; Blake, J.A.; Botstein, D.; Butler, H.; Cherry, J.M.; Davis, A.P.; Dolinski, K.; Dwight, S.S.; Eppig, J.T.; et al. Gene ontology: Tool for the unification of biology. The Gene Ontology Consortium. *Nat. Genet.* **2000**, *25*, 25–29. [CrossRef]
38. Gene Ontology, C.; Aleksander, S.A.; Balhoff, J.; Carbon, S.; Cherry, J.M.; Drabkin, H.J.; Ebert, D.; Feuermann, M.; Gaudet, P.; Harris, N.L.; et al. The Gene Ontology knowledgebase in 2023. *Genetics* **2023**, *224*, iyad031. [CrossRef]
39. Thomas, P.D.; Ebert, D.; Muruganujan, A.; Mushayahama, T.; Albou, L.P.; Mi, H. PANTHER: Making genome-scale phylogenetics accessible to all. *Protein Sci.* **2022**, *31*, 8–22. [CrossRef]
40. Xie, Z.; Bailey, A.; Kuleshov, M.V.; Clarke, D.J.B.; Evangelista, J.E.; Jenkins, S.L.; Lachmann, A.; Wojciechowicz, M.L.; Kropiwnicki, E.; Jagodnik, K.M.; et al. Gene Set Knowledge Discovery with Enrichr. *Curr. Protoc.* **2021**, *1*, e90. [CrossRef]
41. Kanehisa, M.; Furumichi, M.; Sato, Y.; Kawashima, M.; Ishiguro-Watanabe, M. KEGG for taxonomy-based analysis of pathways and genomes. *Nucleic Acids Res.* **2023**, *51*, D587–D592. [CrossRef] [PubMed]
42. Martinotti, S.; Patrone, M.; Manfredi, M.; Gosetti, F.; Pedrazzi, M.; Marengo, E.; Ranzato, E. HMGB1 osteo-modulatory action on osteosarcoma SaOS-2 cell line: An integrated study from biochemical and -omics approaches. *J. Cell. Biochem.* **2016**, *117*, 2559–2569. [CrossRef] [PubMed]
43. Manfredi, M.; Martinotti, S.; Gosetti, F.; Ranzato, E.; Marengo, E. The secretome signature of malignant mesothelioma cell lines. *J. Proteom.* **2016**, *145*, 3–10. [CrossRef] [PubMed]
44. Szklarczyk, D.; Kirsch, R.; Koutrouli, M.; Nastou, K.; Mehryary, F.; Hachilif, R.; Gable, A.L.; Fang, T.; Doncheva, N.T.; Pyysalo, S.; et al. The STRING database in 2023: Protein-protein association networks and functional enrichment analyses for any sequenced genome of interest. *Nucleic Acids Res.* **2023**, *51*, D638–D646. [CrossRef]